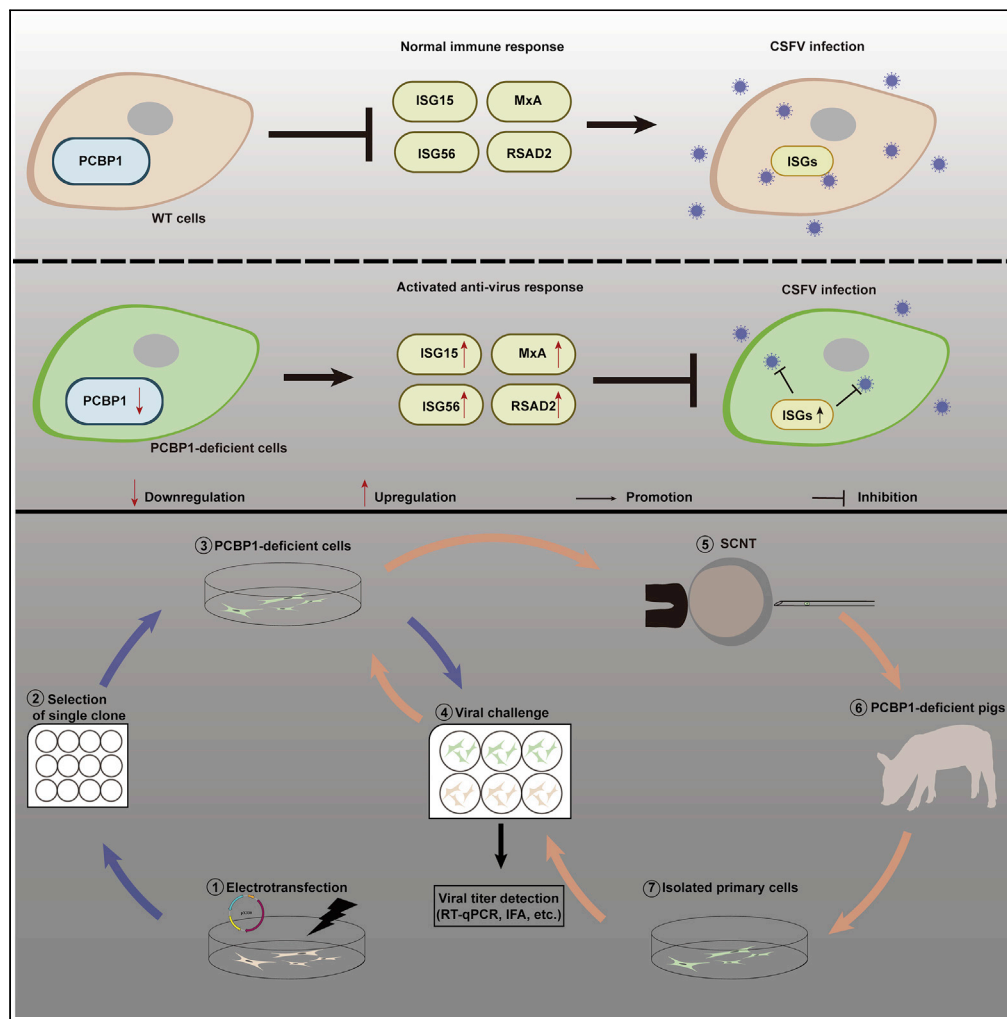


Article

Generation of PCBP1-deficient pigs using CRISPR/Cas9-mediated gene editing



Chunyun Qi, Daxin Pang, Kang Yang, ..., Xiaochun Tang, Hongsheng Ouyang, Zicong Xie

xzc@jlu.edu.cn

Highlights

Reduced CSFV infection in PCBP1-deficient cells is related to activated ISGs expression

PCBP1-deficient pigs were successfully generated via gene-editing technology

Primary cells isolated from PCBP1-deficient pigs exhibited reduced CSFV infection



Article

Generation of PCBP1-deficient pigs using CRISPR/Cas9-mediated gene editing

Chunyun Qi,¹ Daxin Pang,^{1,2,3} Kang Yang,¹ Shuyu Jiao,¹ Heyong Wu,¹ Chuheng Zhao,¹ Lanxin Hu,¹ Feng Li,¹ Jian Zhou,¹ Lin Yang,¹ Dongmei Lv,^{1,2,3} Xiaochun Tang,^{1,2,3} Hongsheng Ouyang,^{1,2,3,4} and Zicong Xie^{1,2,3,5,*}

SUMMARY

Classical swine fever virus (CSFV), a classic swine fever pathogen, causes severe economic losses worldwide. Poly (rC)-binding protein 1 (PCBP1), which interacts with N^{pro} of CSFV, plays a vital role in CSFV growth. We are the first to report the generation of PCBP1-deficient pigs via gene-editing technology. The PCBP1-deficient pigs exhibited normal birth weight and reproductive-performance traits and developed normally. Viral challenge experiments indicated that primary cells isolated from F₀- and F₁-generation pigs exhibited significantly reduced CSFV infection. Additional mechanistic exploration further confirmed that the PCBP1 deficiency-mediated antiviral effect is related to the activation of type I interferon (IFN). Besides showing that a gene-editing strategy could be used to generate PCBP1-deficient pigs, our study introduces a valuable animal model for further investigating the infection mechanisms of CSFV that will help to develop better antiviral solutions.

INTRODUCTION

Classical swine fever (CSF) caused by CSFV, is a highly contagious porcine disease that causes substantial economic losses (Fan et al., 2021; Ma et al., 2019). CSF is generally characterized by high fever, inappetence, and general weakness, followed by neurological deterioration, skin hemorrhage, and splenic infarction (Postel et al., 2018; Zhou, 2019). The genome of CSFV encodes four structural proteins (C, E^{ns}, E1, and E2) and eight nonstructural proteins (N^{pro}, p7, NS3, NS4A, NS4B, NSSA, and NS5B), which utilize host factors to enhance replication and evade cellular immunity (Goraya et al., 2018). The envelope protein, E^{ns}, interacts with heparan sulfate (HS) (Hulst et al., 2000) or laminin receptor (LamR) (Chen et al., 2015) to attach CSFV particles to the surface of permissive cells, and the structural protein E2 interacted with Annexin A2 (Anx2) and/or mitogen-activated protein kinase kinase 2 (MEK2) to promote CSFV production (Li et al., 2017). Recently, N^{pro} was suggested to interact with the host factor PCBP1 to enhance the replication of CSFV (Li et al., 2013).

PCBP1 is an RNA- or DNA-binding protein that can regulate the process of pre-mRNA, mRNA stability, and translation (Choi et al., 2009; Guo and Jia, 2018). It also participates in the formation of the iron chaperone complex, affecting the delivery of iron in cells (Patel et al., 2019). Additionally, PCBP1 deficiency could decrease apoptosis induced by heavily oxidized RNA in human cells (Ishii et al., 2018, 2020). On the other hand, in the virus–host interaction, PCBP1 promotes the binding of cyclic GMP-AMP synthase (cGAS) to DNA in a manner dependent on viral infection, and PCBP1 deficiency can inhibit the cytosolic DNA- and DNA virus-triggered induction of downstream effector genes (Liao et al., 2020). Moreover, PCBP1 can mediate the housekeeping degradation of mitochondrial antiviral signaling (MAVS) via ubiquitination by the E3 ubiquitin ligase atrophin 1-interacting protein 4 (AIP4), and overexpression of PCBP1 inhibits Sendai virus (SeV)-induced antiviral responses (Zhou et al., 2012). Accumulating evidence has shown that PCBP1 can bind the hepatitis C virus (HCV) 5′ untranslated region (UTR) (Fan et al., 2014; Flynn et al., 2015), and the knockdown of PCBP1 decreased HCV RNA proliferation during infection (Choi et al., 2004; Randall et al., 2007). PCBP1 also interacts with porcine reproductive and respiratory syndrome virus (PRRSV) nsp1β and colocalizes with the viral replication and transcription complex (RTC) (Beura et al., 2011). However, confirmation was performed in the Marc-145 cell line, which are not porcine cells. The definitive roles of PCBP1 in the duration of viral infection need to be further investigated in cells or individuals of porcine origin.

Although vaccines have been widely used to control CSFV infection in populations, sporadic infection occurs continuously (Goraya et al., 2018; Li et al., 2017; Luo et al., 2017). To fundamentally counteract the

¹Key Lab for Zoonoses Research, Ministry of Education, Animal Genome Editing Technology Innovation Center, College of Animal Sciences, Jilin University, Changchun, Jilin Province 130062, China

²Chongqing Research Institute, Jilin University, Chongqing 401123, China

³Chongqing Jitang Biotechnology Research Institute Co., Ltd, Chongqing, China

⁴Shenzhen Kingsino Technology Co., Ltd., Shenzhen, China

⁵Lead contact

*Correspondence: xzc@jlu.edu.cn

<https://doi.org/10.1016/j.isci.2022.105268>



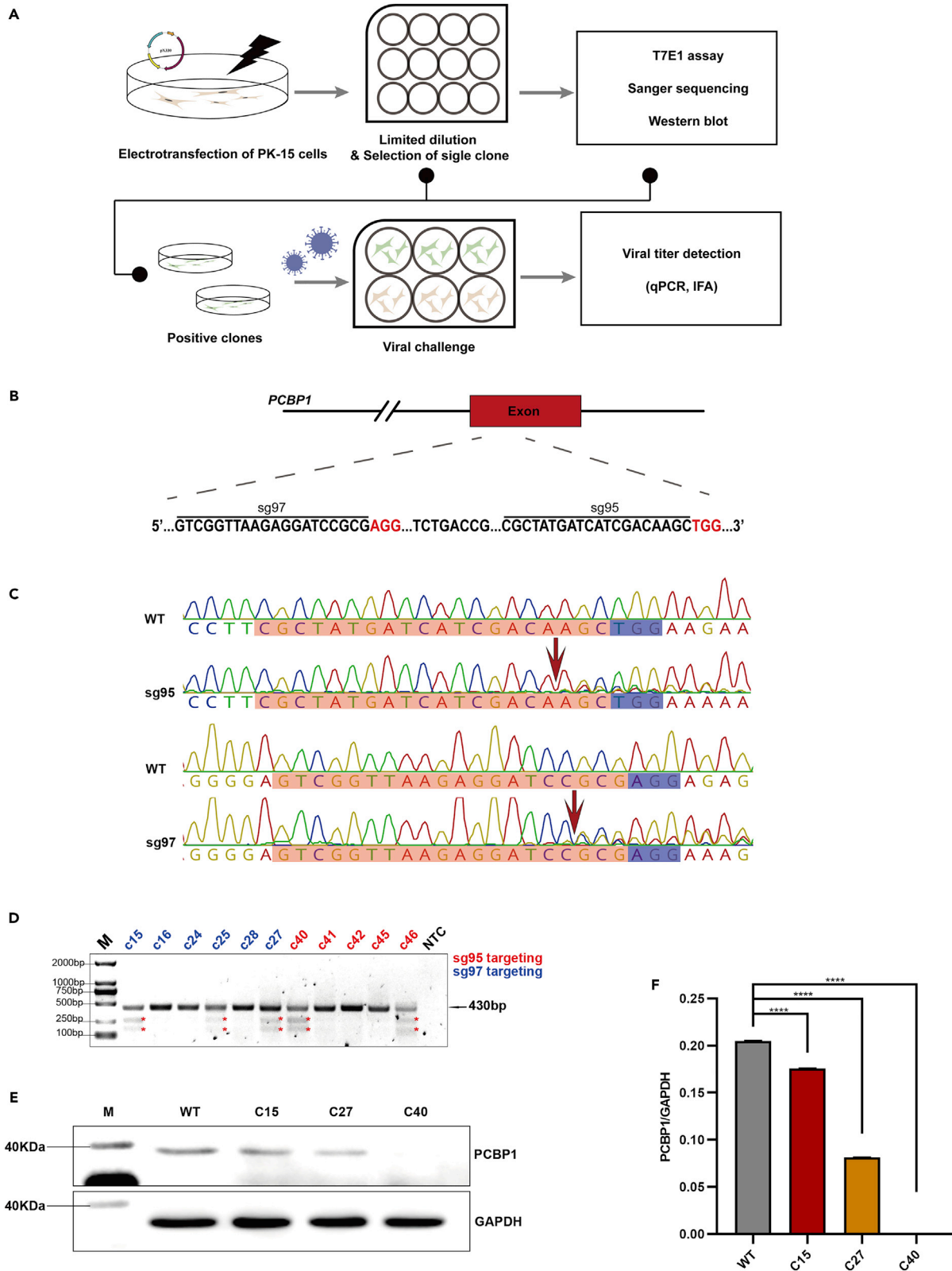


Figure 1. Establishment of PCBP1 KO cells

(A) Schematic diagram of the selection of PCBP1 KO monoclonal clones and experimental design at the cellular level.
(B) A targeting diagram of representative sgRNAs on the PCBP1 locus. The red bases indicate the PAM sequence.
(C) The cleavage efficiency of sg95 and sg97. The pools of PK-15 cells separately transfected with PX330-sg95/sg97 were amplified using specific primers, followed by Sanger sequencing. The nested peaks in the chromatogram near the cleavage site of the Cas9 endonuclease indicated the efficiency of the sgRNAs. The red arrow indicates the cleavage site of the Cas9 protein. The bases in the purple rectangle are PAM sequences. The bases in the orange rectangle are crRNA sequences.
(D) Selection of positive PCBP1 KO clones. The targeting regions on the PCBP1 loci of different clones were amplified, and then the amplicons were cut by T7 endonuclease. The black arrow indicates the band size of the amplicons. Red asterisks indicate the fragments cut by T7 endonuclease. c15, c16, c24, c25, c27, and c28 were selected from the cell pool transfected with PX330-sg97 and are indicated in blue font. c40, c41, c42, c45, and c46 were selected from the cell pool transfected with PX330-sg95 and indicated in red font. The expected sizes of both cleavage fragments in c15, c16, c24, c25, and c27 were approximately 170 and 260 bp, respectively. The expected sizes of both cleavage fragments in c40, c41, c42, c45, and c46 were approximately 150 and 285 bp, respectively.
(E) Representative image of PCBP1 protein levels in c15, c27, and c40. The total-cell lysates of c15, c27, c40, and WT cells were separated using SDS-PAGE, followed by immunoblotting with anti-PCBP1 antibody. GAPDH was used as an internal control. M, protein marker (10–180 kDa).
(F) Gray intensity analysis of PCBP1 using Fiji software. The PCBP1 band intensity was normalized to that of GAPDH in the same sample. Every sample was measured three times by Fiji. Bars are presented as the mean \pm SEM, and data were analyzed using Student's *t*-test using GraphPad Prism 8.0.
**** $p < 0.0001$; ns, no significance; $n = 3$.

consequences of CSFV, genetic strategies complementary to other methods can be adapted. Genetic modification of pigs is an efficacious strategy that has been adopted to generate pigs with resistance to various swine viruses, such as PRRSV (Burkard et al., 2018; Chen et al., 2019) and transmissible gastroenteritis virus (TGEV) (Xu et al., 2020), using CRISPR/Cas9 technology. Hence, based on the host factors hijacked by corresponding viruses, which play critical roles in viral entry, internalization, and replication, creating pigs with viral resistance via the knockout (KO) method may be promising.

In summary, in this proof-of-principle study, we demonstrate that PCBP1 KO/deficiency could significantly inhibit CSFV growth in PK-15 cells and primary porcine fibroblasts. More importantly, our study is the first to report the generation of PCBP1-deficient pigs via gene-editing technology. Viral challenge experiments indicated that primary cells isolated from F₀- and F₁-generation pigs could significantly reduce CSFV infection. In addition, the effect of PCBP1 deficiency on the type I interferon (IFN- α) pathway and predicted interactors of PCBP1 after CSFV infection were explored.

RESULTS**Generation of PCBP1 KO PK-15 cells**

To further confirm the inhibitory effect of PCBP1 on CSFV infection (Figure 1A) and explore the feasibility of generating PCBP1 KO antiviral pigs (Li et al., 2013), the relative expression of PCBP1 in various organs was first elucidated (Figure S1A). According to previous reports on the characteristics of the PCBP1 sequence (Ishii and Sekiguchi, 2019; Zhang et al., 2020), two sgRNAs (sg97 and sg95) were designed to target the N-terminus of the only exon (Figure 1B). The two gRNA-recombined PX330 plasmids were introduced into PK-15 cells using electroporation (Figure 1A). Sanger sequencing of the cell pool electrotransfected with PX330-sg95/sg97 plasmids indicated that both gRNAs could achieve high cleavage efficiency (Figures 1C, S1B, and S1C).

To select PCBP1 KO clones, PX330-sg95 and PX330-sg97 plasmids were separately electrotransfected into PK-15 cells. PCBP1 KO-positive clones were selected with the limited dilution method. As shown in Figure 1D, subset clones were examined through a T7 endonuclease I (T7E1) assay, in which clone 15 (c15), clone 25 (c25), and clone 27 (c27) were shown to be sg97-targeting positive clones, whereas clone 40 (c40) and clone 46 (c46) were sg95-targeting positive clones. The targeting region of the PCBP1 alleles in c15, c27, and c40 was also confirmed using Sanger sequencing (Figure S1D), and the truncated PCBP1 amino acid sequence is displayed in Figure S1E. c15, c27, and c40 were chosen for further research.

Alterations in PCBP1 protein levels in the three positive clones were further assessed using western blotting. As shown in Figure 1E, PCBP1 deficiency occurred not only in the homozygous KO clone (c40) but also in the heterozygous clones (c15 and c27), but this was not observed in the wild-type (WT) PK-15 cells. Furthermore, gray intensity analysis of the corresponding band also indicated that the PCBP1 level in the PCBP1-deficient/KO clones was notably reduced compared with that in the WT cells (Figure 1F).

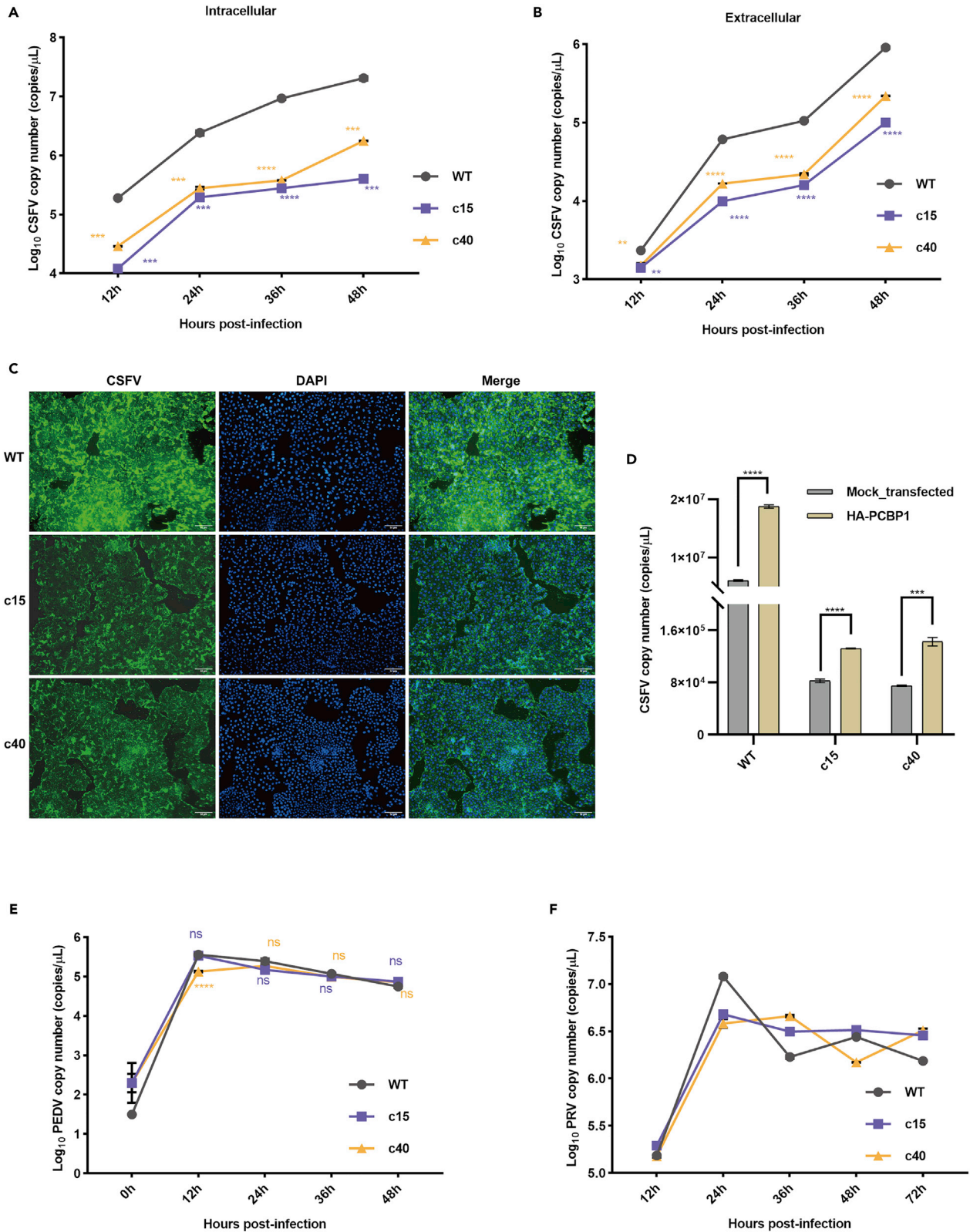


Figure 2. Viral proliferation kinetics in PCBP1-deficient/KO PK-15 cells

(A) The replication kinetics of CSFV in PCBP1 KO/deficient PK-15 cells. WT, c15, and c40 cell cultures were infected with CSFV (MOI = 0.1). At the indicated time after infection, samples were collected, and RT-qPCR was performed to detect the CSFV genome copy number.

(B) Representative images from immunofluorescence assays (IFA) detecting CSFV in CSFV-infected WT, c15, and c40 cells. Cells were seeded in a 24-well plate. After attachment, cell cultures were infected with CSFV (MOI = 1) for 48 h, and then the monolayer was fixed for staining with E2-specific antibody (PAb). Scale bar, 50 μ m.

(C) The extracellular CSFV particle copy number in WT, c15, and c40 cells at various hpi. WT, c15, and c40 cells were infected with CSFV (MOI = 1). At the indicated time after infection, the culture medium was collected and subjected to RT-qPCR.

(D) CSFV genome copy numbers in PCBP1-overexpressing WT, c15, and c40 cells. WT, c15, and c40 cells were transfected with pcDNA3.1-HA-PCBP1-His using polyethyleneimine (PEI). At 48 h post-transfection, cell cultures were infected with CSFV (MOI = 1) for 48 h, and then the monolayer was collected for RT-qPCR.

(E) The replication kinetics of PEDV in PCBP1 KO/deficient PK-15 cells. WT, c15, and c40 cell cultures were infected with PEDV (MOI = 0.01). At the indicated time after infection, samples were collected and RT-qPCR was performed to detect the PEDV genome copy number.

(F) The replication kinetics of PRV in PCBP1 KO/deficient PK-15 cells. WT, c15, and c40 cell cultures were infected with PRV (MOI = 0.01). At the indicated time after infection, samples were collected, and RT-qPCR was performed to detect the CSFV genome copy number. Bars are presented as the mean \pm SEM, and data were analyzed using Student's t-test using GraphPad Prism 8.0. *** p < 0.001; **** p < 0.0001; ns, no significance; n = 3.

PCBP1 KO PK-15 cells inhibit CSFV proliferation but not PRV and PEDV proliferation

Next, to explore the antiviral activity of PCBP1 KO/deficient cells, c15, c40, and WT PK-15 cells were infected with CSFV. RT-qPCR was performed to detect intracellular CSFV particles at various hours postinfection (hpi). As shown in Figure 2A, c15 and c40 had significantly lower CSFV genome copies of CSFV than WT PK-15 cells at 12 hpi (4.084 ± 0.01 and 4.46 ± 0.006 versus 5.277 ± 0.033 log₁₀ copies/ μ L; p < 0.0001). In addition, the most significant difference occurred at 48 hpi for c15 (5.632 ± 0.007 versus 7.307 ± 0.035 log₁₀ copies/ μ L; p < 0.0001) and at 36 hpi for c40 (5.580 ± 0.004 versus 6.966 ± 0.023 log₁₀ copies/ μ L; p < 0.0001). Then, c40, c15, and WT PK-15 cells were infected with CSFV for 48 h before IFA. As shown in Figures 2B and S2A, the detectable CSFV signal in the PCBP1-deficient/KO cells was significantly weaker than that in the WT cells. The CSFV particles in the supernatant also showed a similar tendency. As shown in Figure 2C, extracellular CSFV particles in the supernatants of infected PCBP1-deficient and KO cells were lower than those in WT PK-15 cells. To further clarify the inhibitory effect of PCBP1 deficiency/KO on CSFV infection, rescue experiments were conducted by ectopically expressing PCBP1 in PCBP1-deficient/KO cells. The results showed that the number of CSFV genome copies in PCBP1-overexpressing cells was moderately increased compared with that in the mock-transfected, PCBP1-deficient cells (Figure 2D).

Porcine epidemic diarrhea virus (PEDV) and porcine pseudorabies virus (PRV) are two other economically important viruses in the swine industry. To further investigate whether PCBP1 KO/deficient positive cells could also inhibit PEDV and PRV, c15 and c40 were separately infected with PEDV and PRV. However, viral challenge experiments indicated that the genome copy numbers of PEDV and PRV in PCBP1-deficient/KO cells and WT PK-15 cells were not significantly different (Figures 2E and 2F). These results suggested that PCBP1 deficiency/KO could significantly inhibit CSFV growth but did not affect PEDV or PRV infection in PK-15 cells. Overall, these results further confirmed that PCBP1 is a positive regulator of CSFV replication and that the KO of cellular PCBP1 has an inhibitory effect on the growth of CSFV.

PCBP1 deficiency inhibits CSFV proliferation at the attachment stage

Given the inhibitory effect of PCBP1 deficiency on CSFV infection, we conducted experiments to determine which steps of the CSFV life cycle were diminished. First, PCBP1-deficient cells were used to determine the effect on CSFV binding and entry. The results showed that CSFV relative units were universally decreased in PCBP1-deficient cells at both high and low MOIs, suggesting that PCBP1 is involved in the attachment phase of the CSFV life cycle (Figures 3A and S2B). The numbers of CSFV units in the entry phase may have been comparable between WT and PCBP1-deficient/KO cells at a low MOI because the number of infectious virions among the total viral particles at a low MOI was lower than that at a high MOI with the same inoculum, which led fewer virions entering the cells (Figure S2B). As expected, the replication stage was also inhibited in PCBP1-deficient cells owing to the decreased number of CSFV particles at the binding stage (Figure 3A). Together, these results showed that PCBP1 deficiency/KO inhibits CSFV proliferation by regulating the binding phase of CSFV.

PCBP1 KO potentiates innate antiviral responses stimulated by CSFV in PK-15 cells

To further clarify whether the suppressive effect on CSFV was caused by increased innate immune levels in PCBP1-deficient cells, we detected the relative expression levels of several IFN genes, such as IFN- α

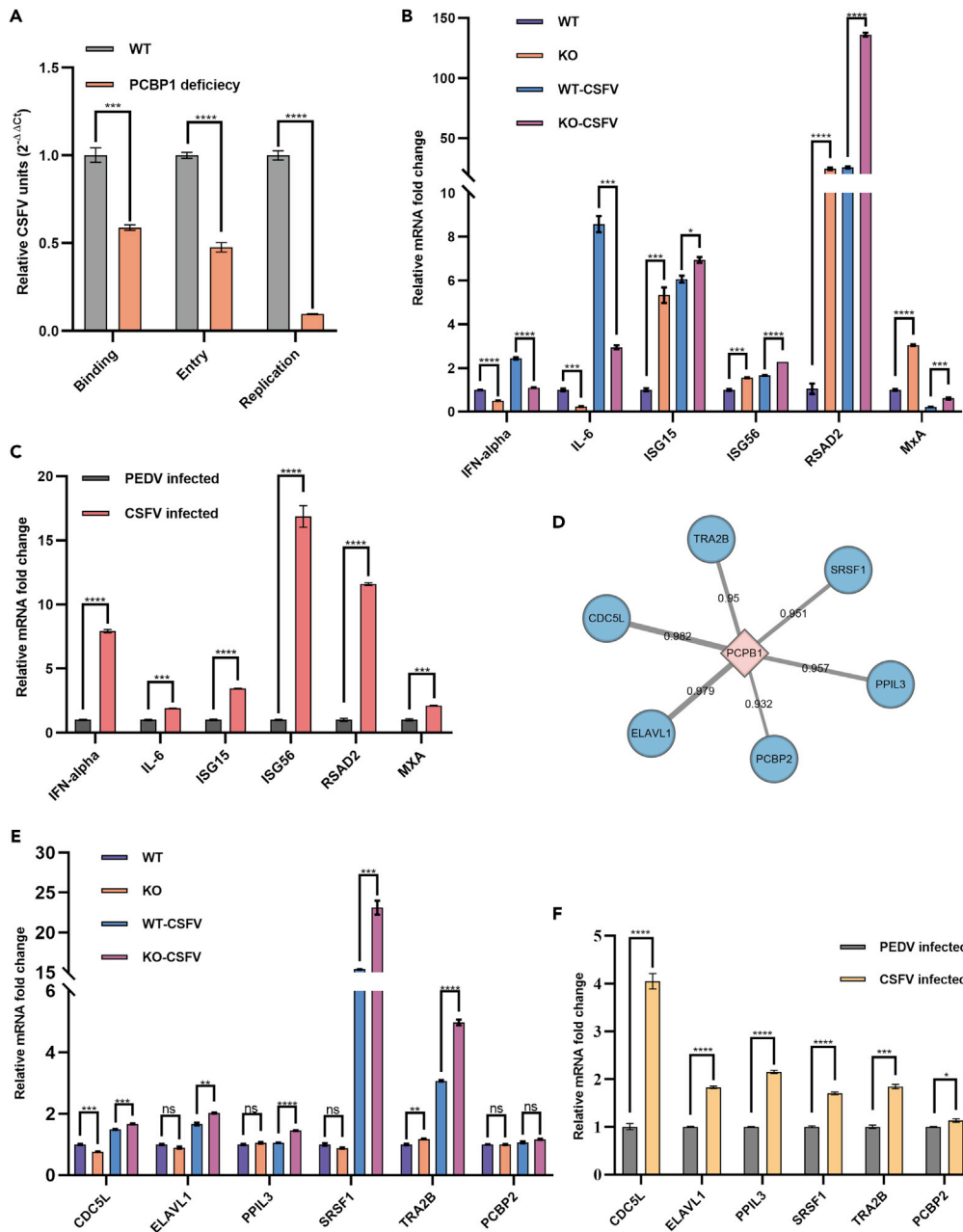


Figure 3. The effect of PCBP1 deficiency on the CSFV life cycle and IFN pathway

(A) Cells were infected with CSFV at a MOI of 10 at 4°C for 1 h and then shifted to 37°C for 0 (binding), 1 (entry), and 24 h (replication). Samples were collected and lysed to determine the number of CSFV RNA units using RT-qPCR.

(B) The relative mRNA fold change of IFN pathway genes and downstream effectors in PCBP1 KO cells.

(C) The relative mRNA fold change in IFN pathway genes and downstream effectors in CSFV-infected PCBP1 KO cells compared with cells infected with PEDV-infected at 48 hpi.

(D) The predicted interactors of PCBP1. The thickness of the gray line represents combined scores.

(E) The relative mRNA fold change of predicted genes in PCBP1 KO cells.

(F) The relative mRNA fold change in predicted genes in CSFV-infected PCBP1 KO cells compared with cells infected with PEDV at 48 hpi. Bars are the mean ± SEM, and the data were analyzed using Student's t-test using GraphPad Prism 8.0.

p* < 0.05; *p* < 0.01; ****p* < 0.001; *****p* < 0.0001; ns, no significance; *n* = 3.

and IL-6, following CSFV infection. Unexpectedly, compared with those in the WT PK-15 groups, the transcription levels of IFN- α and IL-6 in PCBP1-deficient cells were decreased (Figure 3B). However, the expression levels of interferon-stimulated genes (ISGs) that have antiviral activity against a broad range of viruses in PCBP1-deficient cells were significantly increased compared with those in the WT cells regardless of CSFV infection (Figure 3B). These results suggested that PCBP1 deficiency cells were in an anti-CSFV state owing to the upregulation of ISGs. Interestingly, both IFN genes and downstream ISGs in CSFV-infected PCBP1-deficient cells were universally increased compared with those in PEDV-infected cells (Figure 3C). Additionally, to observe the alteration of the network involving PCBP1, we searched for the genes that interact with PCBP1 using the STRING database (Szklarczyk et al., 2016, 2020). The top six predicted genes are shown in Figure 3D. Although the levels of these predicted genes in PCBP1-deficient cells were comparable with the WT cells, these genes were increased following CSFV infection, and especially, serine and arginine-rich splicing factor 1 (SRSF1), transformer 2 beta homolog (TRA2B) were significantly upregulated (Figure 3E). In addition, the transcription levels of these predicted genes in PCBP1-deficient cells were also notably upregulated by CSFV infection compared with PEDV infection (Figure 3F).

Primary fibroblasts derived from PCBP1-deficient pigs diminish CSFV infection

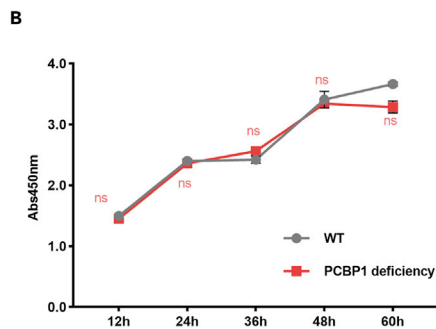
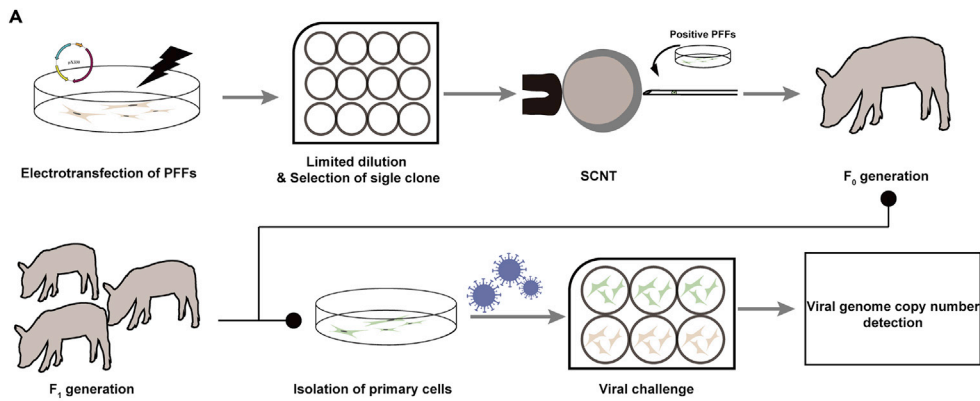
To further estimate the feasibility of producing a PCBP1 KO pig, sg97 was introduced into Large white porcine fetal fibroblasts (PFFs), and PCBP1-deficient PFFs were selected via the limited dilution method (Figure 4A). The CCK-8 assay was first employed to monitor the viability of PCBP1-deficient PFFs. As shown in Figure 4B, the CCK-8 results indicated that PCBP1 deficiency in PFFs did not induce significant adverse effects. Before somatic cell nuclear transfer (SCNT), we determined blastocyst development, and PCBP1-deficient PFFs showed a blastocyst morphology and development rates comparable with those of WT PFFs (Figures S3A and S3B). Next, PCBP1-deficient PFFs were selected as donor cells for SCNT, and a total of 921 mature reconstructed embryos were transferred into five surrogates. The piglets were born after approximately 114 days of pregnancy, and three were identified as positive heterozygous PCBP1-deficient pigs using PCR, which was further confirmed using Sanger sequencing (Figures 4C and 4D). The predicted amino acid sequence of the PCBP1-deficient piglets is shown in Figure S3C. To evaluate whether off-target effects were present in these PCBP1-deficient pigs, eight potential off-target sites (OTs) on different chromosomes were predicted using RGEN tools (<http://www.rgenome.net/cas-offfinder/>), and no obvious off-target events occurred, as shown in Figures S4A and S4B.

When the PCBP1-deficient founders were sexually mature, we obtained seven F1-generation piglets by crossing the PCBP1-deficient founders with WT pigs. Three of these piglets were PCBP1-deficient offspring, and four were WT offspring. To further verify their ability to resist CSFV infection, primary fibroblasts isolated from the tail tips of the PCBP1-deficient F0 and F1 pigs were infected with CSFV. Compared with that in WT fibroblasts, IFA results indicated that fibroblasts derived from the F₀- and F₁-generation PCBP1-deficient pigs could effectively decrease CSFV infection (Figures 5A and 5B). The number of extracellular CSFV particles in the supernatants of CSFV-infected fibroblasts isolated from the PCBP1-deficient pigs also confirmed this inhibitory effect (Figure 5C).

DISCUSSION

Infection with CSFV, the pathogen that causes CSF, which is characterized by multiple hemorrhages, leukopenia, high fever, abortion, and neurological dysfunction (Fan et al., 2021; Zheng et al., 2020), has caused significant economic losses worldwide. The production of genetically modified pigs is an efficacious strategy to limit viral infection and different types of genetically modified pigs with resistance to porcine viruses have been generated through this strategy (Hu et al., 2015b; Huang et al., 2017; Lu et al., 2017; Xie et al., 2020a; Yan et al., 2014; Zhao et al., 2016). In this report, we targeted the PCBP1 locus in the porcine genome using CRISPR/Cas9 technology and successfully acquired PCBP1 KO/deficient PK-15 cells and PCBP1-deficient pigs. viral challenge experiments both *in vitro* and *ex vivo* illustrated that PCBP1 KO/efficient cells showed significantly reduced CSFV infection. To the best of our knowledge, this study is the first report of PCBP1-deficient pigs with potential resistance to CSFV.

A previous study reported that mice heterozygous for PCBP1 display a mild and nondisruptive defect in initial postpartum weight (Ghanem et al., 2016). In this study, the F₀- and F₁-generation PCBP1-deficient pigs exhibited a normal birth weight and phenotype, demonstrating that PCBP1 plays different roles in developmental regulation in mice and pigs. In our study, *in vitro* CSFV challenge experiments indicated that PCBP1 deficiency/KO could significantly inhibit CSFV growth in PK-15 cells and that the rescue of



D

```

#590  GAAAGGGGAGTCGGTTAAGAGGATCCGCGAGGAGAGTGGC  +/+
      GAAAGGGGAGTCGGTTAAGAGGATCCGCGAGGAGAGTGGC

#592  GAAAGGGGAGTCGGTTAAGAGGATCCGCGAGGAGAGTGGC  -/+
      GAAAGGGGAGTCGGTTAACAGG-----GAGAGTGGC

#594  GAAAGGGGAGTCGGTTAAGAGGATCCGCGAGGAGAGTGGC  -/+
      GAAAGGGGAGTCGGTTAACAGG-----GAGAGTGGC

#596  GAAAGGGGAGTCGGTTAAGAGGATCCGCGAGGAGAGTGGC  -/+
      GAAAGGGGAGTCGGTTAACAGG-----GAGAGTGGC
    
```

Figure 4. Production of PCBP1-deficient pigs

(A) Schematic diagram of the production of PCBP1-deficient pigs using somatic cell nuclear transfer (SCNT) and the experimental design of ex vivo viral challenge.

(B) Cell viability of PCBP1-deficient PFFs. PCBP1-deficient PFFs and WT cells were seeded in 96-well plates. After attachment, CCK8 working solution was added to the culture medium. The absorbance at 450 nm was detected after incubation for 2 h.

(C) Photograph of the F₀ generation of PCBP1-deficient piglets.

(D) T-cloning and Sanger sequencing of the *PCBP1* alleles of F₀ piglets. The targeting region on the *PCBP1* locus was amplified, and then the amplicons were ligated into T vectors. Seven colonies were selected for sequencing. PAM sites are highlighted in red. Indels are shown in yellow. #590, #592, #594, and #596 were the codes for the individual litters of the surrogate. +/+ , WT pig; -/+ , heterozygous PCBP1-deficient pigs. Bars show the mean \pm SEM and the data were analyzed using Student's t-test using GraphPad Prism 8.0. ns, no significance; n = 3.

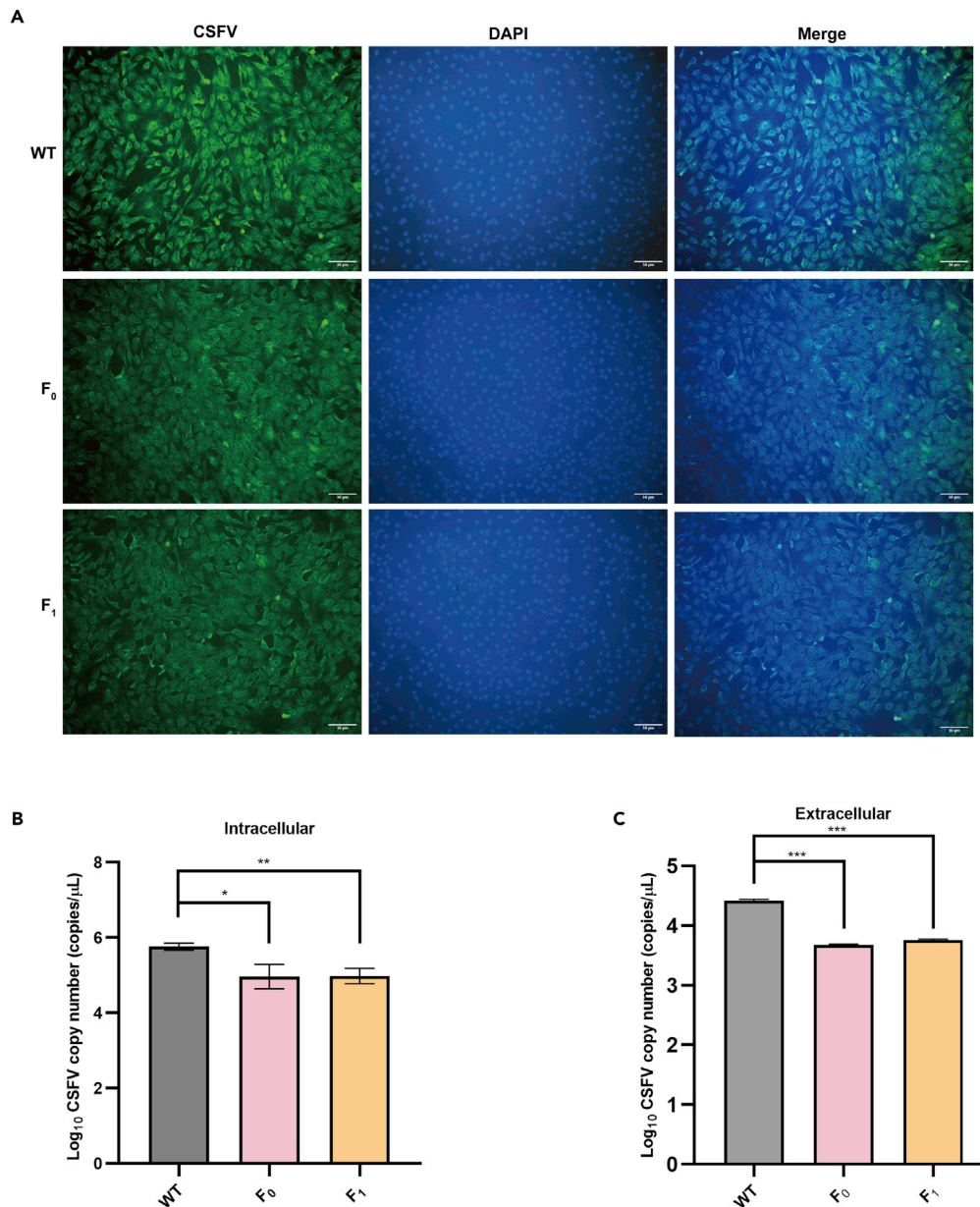


Figure 5. Growth of CSFV in primary fibroblasts isolated from PCBP1-deficient pigs

(A) Representative IFA images of CSFV in CSFV-infected fibroblasts. Primary fibroblasts isolated from the WT and F₀- and F₁-generation were seeded in a 24-well plate. After attachment, cell cultures were infected with CSFV (MOI = 1) for 48 h. The monolayer was fixed and probed with E2-specific antibody (PAb), and the supernatants were collected to determine the CSFV copy number using RT-qPCR. Scale bar, 50 μm.

(B) Intracellular CSFV particles in primary fibroblasts isolated from the F₀- and F₁-generation PCBP1-deficient pigs. The isolated primary fibroblasts were seeded in a six-well plate. The cell cultures were infected with CSFV (MOI = 1) for 48 h. The cell pellets were collected to determine the intracellular CSFV particle number.

(C) Extracellular CSFV particles in primary fibroblasts isolated from the F₀- and F₁-generation PCBP1-deficient pigs. Primary cells isolated from pig tails were seeded in a 24-well plate. The cell cultures were infected with CSFV (MOI = 1) for 48 h, and the supernatants were collected to determine the extracellular CSFV copy number. Bars show the mean ± SEM, and the data were analyzed using Student's t-test using GraphPad Prism 8.0. **p* < 0.05; ***p* < 0.01; *n* = 3.

PCBP1 expression could weaken this suppressive effect. CSFV growth may not have been restored to levels comparable with those of the WT cells owing to the low transfection efficacy (approximately 10–15%) (data not shown). Notably, primary fibroblasts isolated from PCBP1-deficient pigs were also resistant to CSFV

infection. The reduction in CSFV in PCBP1-deficient fibroblasts may have been less than that in PCBP1-deficient PK-15 cells because the primary fibroblasts gradually aged over cell passages, as this cell line is not immortal, or because the cell type and culture conditions differed between PK-15 cells and primary fibroblasts. Based on the consistency of this suppressive effect at the cellular (through gene editing) and individual levels (Hu et al., 2015a; Xie et al., 2018), PCBP1 KO pigs show promise in their resistance to CSFV. However, the reduction in CSFV copy number in the PCBP1-deficient cells could not be transferred into *in vivo* clinical results owing to the limited number of PCBP1-deficient pigs. CSFV challenge will be administered until the herd of PCBP1-deficient pigs is large enough for *in vivo* viral challenge. Otherwise, considering the similarity between CSFV and other pestiviruses, whether PCBP1 deficiency could influence other pestiviruses may need more detailed investigations.

A previous report proposed that the deletion of KHIII on the C-terminus of PCBP1 abolished the PCBP1–N^{pro} interaction (Li et al., 2013). However, the ability of fibroblasts in which three amino acid (9 bp) in the PCBP1 N-terminus were deleted to resist CSFV infection suggests that the key amino acids involved in CSFV infection may also exist in the KHI domain of PCBP1. Although KHIII of PCBP1 is important for the PCBP1–N^{pro} interaction, this interaction may not be the only manner in which PCBP1 affects CSFV infection. Some unrevealed mechanisms relevant to PCBP1 still need to be explored. Recently, screening of a base editing library derived from CRISPR/Cas9 technology has been rapidly developed at a high speed, and this strategy has been widely used (Arbab et al., 2020; Cuella-Martin et al., 2021; Hanna et al., 2021). Comprehensive screening of the precise amino acids in PCBP1 with saturated editing is expected to address the specific sites involved in CSFV infection and explore targeted drugs.

To reveal the effect of PCBP1 deficiency on CSFV infection and clarify how PCBP1 deficiency could inhibit CSFV proliferation, we determined which phase of the CSFV infection cycle was affected by PCBP1 deficiency and monitored the level of innate immunity-related transcripts. Our results showed that the subsequent internalization and replication of CSFV in PCBP1-deficient cells were expectedly inhibited owing to the decreased copy number of CSFV at the binding stage. However, the exact mechanism by which PCBP1 affects the interaction of surface host proteins with CSFV still needs further elucidation. Type I IFN has antiviral activity, and RNA viruses of the family Flaviviridae are sensitive to type I IFN (Goraya et al., 2018; Schneider et al., 2014). In addition, activation of type I IFN can induce the synthesis of hundreds of proteins, such as ISGs (Li et al., 2020; Schneider et al., 2014), including ISG15, ISG56, and RSAD2, all of which are well documented to inhibit a broad spectrum of viruses (Helbig et al., 2013; Li et al., 2020; Raychoudhuri et al., 2011; Van der Hoek et al., 2017; Xie et al., 2020b). It was suggested that CSFV N^{pro} is involved in the inhibition of type I IFN by interacting with IRF3 (Bauhofer et al., 2007; Gottipati et al., 2016). In terms of the literature and inhibitory effect of PCBP1 KO cells on CSFV, we wondered if the innate immunity-related transcripts levels in PCBP1 KO cells would be higher than those in WT cells following CSFV infection. To this end, we determined the relative expression of IFN genes and ISGs after CSFV infection. Our data demonstrated that although the levels of type I IFN genes were decreased, the levels of downstream ISGs were increased in PCBP1 KO PK-15 cells regardless of CSFV infection, implying enhanced innate cellular immunity. In addition, compared with uninfected PCBP1 KO groups, we found that these upregulated ISGs were increased further in CSFV-infected PCBP1 KO PK-15 cells. These findings revealed that reduced CSFV infection was related to PCBP1 deficiency-mediated ISGs upregulation. Similarly, a previous report illustrated that knockdown of PCBP1 promoted an increase in type I IFN in cells infected with SeV or transfected with poly (I:C) (Zhou et al., 2012), which partly supports our finding. Next, the finding that the transcript levels of IFN genes and ISGs stimulated by CSFV in PCBP1-deficient cells were higher than those elicited by PEDV also explains the finding that PCBP1-deficient cells could inhibit CSFV but not PEDV. A number of PEDV structural and nonstructural proteins (E, M, N, nsp1, nsp3, nsp7, nsp8, nsp14, nsp15, and nsp16) were confirmed to play a role in regulating the immune response, which involves sophisticated signaling pathways (Hu et al., 2021). Therefore, an in-depth investigation of these PEDV proteins, host factors, and their interactions is needed. The above findings suggest that CSFV and PEDV are quite different with respect to their sensitivity to PCBP1.

To further explore the inhibitory effect of PCBP1 deficiency/KO on CSFV infection, we predicted PCBP1 interactors using the STRING database (STRING: functional protein association networks (string-db.org)). Compared with those in the WT group, cell division cycle 5 like (CDC5 L), ELAV-like RNA-binding protein 1 (ELAVL1), peptidylprolyl isomerase like three (PPI3), SRSF1, TRA2B, and PCBP2 levels were universally upregulated following CSFV infection in the PCBP1 KO group, suggesting that these predicted factors

are important factors that coregulate PCBP1-related antiviral activity. In addition, the finding that the transcript levels of these predicted factors in CSFV-infected PCBP1-deficient cells were higher than those in PEDV-infected cells further confirmed our above hypothesis.

More importantly, we ultimately demonstrated that PCBP1-deficient PFFs could be used to generate PCBP1-deficient pigs via SCNT, and recently, PCBP1-deficient pigs of the F₁ generation, the offspring of heterozygous pig #592, were successfully produced. Compared with littermate WT piglets, F₀- and F₁-generation PCBP1-deficient piglets exhibited a normal birth weight and phenotype, and viral challenge experiments indicated that fibroblasts isolated from F₀- and F₁-generation PCBP1-deficient pigs exhibited marked resistance to CSFV infection. These results suggested that the acquired PCBP1 deficiency-based ability in these F₀-generation founders to resist viral infection could be stably transmitted to their F₁-generation offspring. Regrettably, the first litter was so small that systematic animal challenge experiments could not be performed. Therefore, it is important to assess potential hazards concerning PCBP1 deficiency/KO. We are conducting long-term studies to monitor antiviral ability, reproductive capability, and growth.

In summary, we demonstrated that PCBP1-deficient pigs were successfully bred using CRISPR/Cas9 technology; these pigs could serve as a valuable animal model for further antiviral research and enrich our understanding of PCBP1 function.

Limitations of the study

We are the first to report the generation of PCBP1-deficient pigs via gene-editing technology, and viral challenge experiments indicated that primary cells isolated from F₀- and F₁-generation pigs exhibited significantly reduced CSFV infection. However, the efficacy of PCBP1 KO/deficiency has not been yet determined against other pestiviruses. Besides, the efficacy of PCBP1-deficient pigs against CSFV needs further investigation.

STAR★METHODS

Detailed methods are provided in the online version of this paper and include the following:

- KEY RESOURCES TABLE
- RESOURCE AVAILABILITY
 - Lead contact
 - Materials availability
 - Data and code availability
- EXPERIMENTAL MODEL AND SUBJECT DETAILS
 - Cells and viruses
- METHOD DETAILS
 - Plasmid construction
 - Electroporation and generation of knock out cell clones
 - T7E1 assay
 - Virus infection
 - Plasmids transfection
 - Viral genome extraction and real-time quantitative PCR
 - Western Blot
 - Binding, entry, and replication assay
 - IFA
 - SCNT
 - Isolation of primary porcine fibroblast
 - Cell viability assay
- QUANTIFICATION AND STATISTICAL ANALYSIS

SUPPLEMENTAL INFORMATION

Supplemental information can be found online at <https://doi.org/10.1016/j.isci.2022.105268>.

ACKNOWLEDGMENTS

This work was financially supported through grants from the Special Funds for Cultivation and Breeding of New Transgenic Organisms (No. 2016ZX08006003), the Scientific Research Project of Education

Department of Jilin Province (Grant No. JJKH20221040KJ), the Shenzhen Key Technology Projects (JSGG20180507182028625), and the Scientific Research Project of Education Department of Jilin Province (Grant No. JJKH20220971KJ).

AUTHOR CONTRIBUTIONS

Overall design of the study and conceptualization, Z.C.X., D.X.P., H.S.O.Y., X.C.T., D.M.L.; funding acquisition: H.S.O.Y., Z.C.X., D.M.L.; experiments and analyses, C.Y.Q., D.X.P., K.Y., S.Y.J., H.Y.W., C.H.Z., L.X.H., F.L., J.Z., L.Y.; writing – original draft, C.Y.Q., Z.C.X.; writing – review and editing, all authors.

DECLARATION OF INTERESTS

The authors declare no competing interests.

Received: March 15, 2022

Revised: July 16, 2022

Accepted: September 29, 2022

Published: October 21, 2022

REFERENCES

- Arbab, M., Shen, M.W., Mok, B., Wilson, C., Matuszek, Z., Cassa, C.A., and Liu, D.R. (2020). Determinants of base editing outcomes from target library analysis and machine learning. *Cell* 182, 463–480.e30. <https://doi.org/10.1016/j.cell.2020.05.037>.
- Bauhofer, O., Summerfield, A., Sakoda, Y., Tratschin, J.D., Hofmann, M.A., and Ruggli, N. (2007). Classical swine fever virus Npro interacts with interferon regulatory factor 3 and induces its proteasomal degradation. *J. Virol.* 81, 3087–3096. <https://doi.org/10.1128/JVI.02032-06>.
- Beura, L.K., Dinh, P.X., Osorio, F.A., and Pattnaik, A.K. (2011). Cellular poly(d) binding proteins 1 and 2 interact with porcine reproductive and respiratory syndrome virus nonstructural protein 1beta and support viral replication. *J. Virol.* 85, 12939–12949. <https://doi.org/10.1128/JVI.05177-11>.
- Burkard, C., Opiessnig, T., Mileham, A.J., Stadejek, T., Ait-Ali, T., Lilloco, S.G., Whitelaw, C.B.A., Archibald, A.L., and Gallagher, T. (2018). Pigs lacking the scavenger receptor cysteine-rich domain 5 of CD163 are resistant to porcine reproductive and respiratory syndrome virus 1 infection. *J. Virol.* 92, e00415–e00418. <https://doi.org/10.1128/JVI.00415-18>.
- Chen, J., He, W.-R., Shen, L., Dong, H., Yu, J., Wang, X., Yu, S., Li, Y., Li, S., Luo, Y., et al. (2015). The laminin receptor is a cellular attachment receptor for classical swine fever virus. *J. Virol.* 89, 4894–4906. <https://doi.org/10.1128/JVI.00019-15>.
- Chen, J., Wang, H., Bai, J., Liu, W., Liu, X., Yu, D., Feng, T., Sun, Z., Zhang, L., Ma, L., et al. (2019). Generation of pigs resistant to highly pathogenic-porcine reproductive and respiratory syndrome virus through gene editing of CD163. *Int. J. Biol. Sci.* 15, 481–492. <https://doi.org/10.7150/ijbs.25862>.
- Choi, H.S., Hwang, C.K., Song, K.Y., Law, P.Y., Wei, L.N., and Loh, H.H. (2009). Poly(C)-binding proteins as transcriptional regulators of gene expression. *Biochem. Biophys. Res. Commun.* 380, 431–436. <https://doi.org/10.1016/j.bbrc.2009.01.136>.
- Choi, K., Kim, J.H., Li, X., Paek, K.Y., Ha, S.H., Ryu, S.H., Wimmer, E., and Jang, S.K. (2004). Identification of cellular proteins enhancing activities of internal ribosomal entry sites by competition with oligodeoxynucleotides. *Nucleic Acids Res.* 32, 1308–1317. <https://doi.org/10.1093/nar/gkh300>.
- Cuella-Martin, R., Hayward, S.B., Fan, X., Chen, X., Huang, J.W., Tagliatala, A., Leuzzi, G., Zhao, J., Rabadan, R., Lu, C., et al. (2021). Functional interrogation of DNA damage response variants with base editing screens. *Cell* 184, 1081–1097.e19. <https://doi.org/10.1016/j.cell.2021.01.041>.
- Fan, B., Lu, K.Y., Raymond Sutandy, F.X., Chen, Y.W., Konan, K., Zhu, H., Kao, C.C., and Chen, C.S. (2014). A human proteome microarray identifies that the heterogeneous nuclear ribonucleoprotein K (hnRNP K) recognizes the 5' terminal sequence of the hepatitis C virus RNA. *Mol. Cell. Proteomics* 13, 84–92. <https://doi.org/10.1074/mcp.M113.031682>.
- Fan, J., Liao, Y., Zhang, M., Liu, C., Li, Z., Li, Y., Li, X., Wu, K., Yi, L., Ding, H., et al. (2021). Anti-Classical swine fever virus strategies. *Microorganisms* 9, 761.
- Flynn, R.A., Martin, L., Spitale, R.C., Do, B.T., Sagan, S.M., Zarnegar, B., Qu, K., Khavari, P.A., Quake, S.R., Sarnow, P., and Chang, H.Y. (2015). Dissecting noncoding and pathogen RNA-protein interactomes. *RNA* 21, 135–143. <https://doi.org/10.1261/rna.047803.114>.
- Ghanem, L.R., Kromer, A., Silverman, I.M., Chatterji, P., Traxler, E., Penzo-Mendez, A., Weiss, M.J., Stanger, B.Z., and Liebhaber, S.A. (2016). The poly(C) binding protein Pcbp2 and its retrotransposed derivative Pcbp1 are independently essential to mouse development. *Mol. Cell Biol.* 36, 304–319. <https://doi.org/10.1128/MCB.00936-15>.
- Goaraya, M.U., Ziaghum, F., Chen, S., Raza, A., Chen, Y., and Chi, X. (2018). Role of innate immunity in pathophysiology of classical swine fever virus infection. *Microb. Pathog.* 119, 248–254. <https://doi.org/10.1016/j.micpath.2018.04.020>.
- Gottipati, K., Holthausen, L.M.F., Ruggli, N., and Choi, K.H. (2016). Pestivirus Npro directly interacts with interferon regulatory factor 3 monomer and dimer. *J. Virol.* 90, 7740–7747. <https://doi.org/10.1128/JVI.00318-16>.
- Guo, J., and Jia, R. (2018). Splicing factor poly(rC)-binding protein 1 is a novel and distinctive tumor suppressor. *J. Cell. Physiol.* 234, 33–41. <https://doi.org/10.1002/jcp.26873>.
- Hanna, R.E., Hegde, M., Fagre, C.R., DeWeirdt, P.C., Sangree, A.K., Szegetles, Z., Griffith, A., Feeley, M.N., Sanson, K.R., Baidi, Y., et al. (2021). Massively parallel assessment of human variants with base editor screens. *Cell* 184, 1064–1080.e20. <https://doi.org/10.1016/j.cell.2021.01.012>.
- Helbig, K.J., Carr, J.M., Calvert, J.K., Wati, S., Clarke, J.N., Eyre, N.S., Narayana, S.K., Fiches, G.N., McCartney, E.M., and Beard, M.R. (2013). Viperin is induced following dengue virus type-2 (DENV-2) infection and has anti-viral actions requiring the C-terminal end of viperin. *PLoS Negl. Trop. Dis.* 7, e2178. <https://doi.org/10.1371/journal.pntd.0002178>.
- Hu, S., Qiao, J., Fu, Q., Chen, C., Ni, W., Wujiayu, S., Ma, S., Zhang, H., Sheng, J., Wang, P., et al. (2015a). Transgenic shRNA pigs reduce susceptibility to foot and mouth disease virus infection. *Elife* 4, e06951. <https://doi.org/10.7554/eLife.06951>.
- Hu, S., Qiao, J., Fu, Q., Chen, C., Ni, W., Wujiayu, S., Ma, S., Zhang, H., Sheng, J., Wang, P., et al. (2015b). Transgenic shRNA pigs reduce susceptibility to foot and mouth disease virus infection. *Elife* 4, e06951. <https://doi.org/10.7554/eLife.06951>.
- Hu, Y., Xie, X., Yang, L., and Wang, A. (2021). A comprehensive view on the host factors and viral proteins associated with porcine epidemic diarrhea virus infection. *Front. Microbiol.* 12, 762358. <https://doi.org/10.3389/fmicb.2021.762358>.
- Huang, G., Liu, X., Tang, X., Du, L., Feng, W., Hu, X., Zhu, L., Li, Q., and Suo, X. (2017). Increased neutralizing antibody production and

- interferon-gamma secretion in response to porcine reproductive and respiratory syndrome virus immunization in genetically modified pigs. *Front. Immunol.* 8, 1110. <https://doi.org/10.3389/fimmu.2017.01110>.
- Hulst, M.M., van Gennip, H.G., and Moormann, R.J. (2000). Passage of classical swine fever virus in cultured swine kidney cells selects virus variants that bind to heparan sulfate due to a single amino acid change in envelope protein E^{ms}. *J. Virol.* 74, 9553–9561. <https://doi.org/10.1128/JVI.74.20.9553-9561.2000>.
- Ishii, T., Hayakawa, H., Igawa, T., Sekiguchi, T., and Sekiguchi, M. (2018). Specific binding of PCBP1 to heavily oxidized RNA to induce cell death. *Proc. Natl. Acad. Sci. USA* 115, 6715–6720. <https://doi.org/10.1073/pnas.1806912115>.
- Ishii, T., Igawa, T., Hayakawa, H., Fujita, T., Sekiguchi, M., and Nakabeppu, Y. (2020). PCBP1 and PCBP2 both bind heavily oxidized RNA but cause opposing outcomes, suppressing or increasing apoptosis under oxidative conditions. *J. Biol. Chem.* 295, 12247–12261. <https://doi.org/10.1074/jbc.RA119.011870>.
- Ishii, T., and Sekiguchi, M. (2019). Two ways of escaping from oxidative RNA damage: selective degradation and cell death. *DNA Repair* 81, 102666. <https://doi.org/10.1016/j.dnarep.2019.102666>.
- Lai, L., Kolber-Simonds, D., Park, K.-W., Cheong, H.-T., Greenstein, J.L., Im, G.-S., Samuel, M., Bonk, A., Rieke, A., Day, B.N., et al. (2002). Production of α -1, 3-galactosyltransferase knockout pigs by nuclear transfer cloning. *Science* 295, 1089–1092. <https://doi.org/10.1126/science.1068228>.
- Li, C., Wang, Y., Zheng, H., Dong, W., Lv, H., Lin, J., Guo, K., and Zhang, Y. (2020). Antiviral activity of ISG15 against classical swine fever virus replication in porcine alveolar macrophages via inhibition of autophagy by ISGylating BECN1. *Vet. Res.* 51, 22. <https://doi.org/10.1186/s13567-020-00753-5>.
- Li, D., Li, S., Sun, Y., Dong, H., Li, Y., Zhao, B., Guo, D., Weng, C., and Qiu, H.J. (2013). Poly(C)-binding protein 1, a novel N(pro)-interacting protein involved in classical swine fever virus growth. *J. Virol.* 87, 2072–2080. <https://doi.org/10.1128/JVI.02807-12>.
- Li, L.-F., Yu, J., Li, Y., Wang, J., Li, S., Zhang, L., Xia, S.-L., Yang, Q., Wang, X., Yu, S., et al. (2016). Guanylate-binding protein 1, an interferon-induced GTPase, exerts an antiviral activity against classical swine fever virus depending on its GTPase activity. *J. Virol.* 90, 4412–4426. <https://doi.org/10.1128/JVI.02718-15>.
- Li, S., Wang, J., Yang, Q., Naveed Anwar, M., Yu, S., and Qiu, H.-J. (2017). Complex virus–host interactions involved in the regulation of classical swine fever virus replication: a minireview. *Viruses* 9, 171.
- Liao, C.Y., Lei, C.Q., and Shu, H.B. (2020). PCBP1 modulates the innate immune response by facilitating the binding of cGAS to DNA. *Cell. Mol. Immunol.* 18, 2334–2343. <https://doi.org/10.1038/s41423-020-0462-3>.
- Lu, T., Song, Z., Li, Q., Li, Z., Wang, M., Liu, L., Tian, K., and Li, N. (2017). Overexpression of histone deacetylase 6 enhances resistance to porcine reproductive and respiratory syndrome virus in pigs. *PLoS One* 12, e0169317. <https://doi.org/10.1371/journal.pone.0169317>.
- Luo, Y., Ji, S., Liu, Y., Lei, J.-L., Xia, S.-L., Wang, Y., Du, M.-L., Shao, L., Meng, X.-Y., Zhou, M., et al. (2017). Isolation and characterization of a moderately virulent classical swine fever virus emerging in China. *Transbound. Emerg. Dis.* 64, 1848–1857. <https://doi.org/10.1111/tbed.12581>.
- Ma, S.-m., Mao, Q., Yi, L., Zhao, M.-q., and Chen, J.-d. (2019). Apoptosis, autophagy, and pyroptosis: immune escape strategies for persistent infection and pathogenesis of classical swine fever virus. *Pathogens* 8, 239.
- Patel, S.J., Frey, A.G., Palenchar, D.J., Achar, S., Bullough, K.Z., Vashisht, A., Wohlschlegel, J.A., and Philpott, C.C. (2019). A PCBP1-BolA2 chaperone complex delivers iron for cytosolic [2Fe-2S] cluster assembly. *Nat. Chem. Biol.* 15, 872–881. <https://doi.org/10.1038/s41589-019-0330-6>.
- Postel, A., Austermann-Busch, S., Petrov, A., Moennig, V., and Becher, P. (2018). Epidemiology, diagnosis and control of classical swine fever: recent developments and future challenges. *Transbound. Emerg. Dis.* 65, 248–261. <https://doi.org/10.1111/tbed.12676>.
- Randall, G., Panis, M., Cooper, J.D., Tellinghuisen, T.L., Sukhodolets, K.E., Pfeffer, S., Landthaler, M., Landgraf, P., Kan, S., Lindenbach, B.D., et al. (2007). Cellular cofactors affecting hepatitis C virus infection and replication. *Proc. Natl. Acad. Sci. USA* 104, 12884–12889. <https://doi.org/10.1073/pnas.0704894104>.
- Raychoudhuri, A., Shrivastava, S., Steele, R., Kim, H., Ray, R., and Ray, R.B. (2011). ISG56 and IFITM1 proteins inhibit hepatitis C virus replication. *J. Virol.* 85, 12881–12889. <https://doi.org/10.1128/JVI.05633-11>.
- Schneider, W.M., Chevillotte, M.D., and Rice, C.M. (2014). Interferon-stimulated genes: a complex web of host defenses. *Annu. Rev. Immunol.* 32, 513–545. <https://doi.org/10.1146/annurev-immunol-032713-120231>.
- Szklarczyk, D., Gable, A.L., Nastou, K.C., Lyon, D., Kirsch, R., Pyysalo, S., Doncheva, N.T., Legeay, M., Fang, T., Bork, P., et al. (2020). The STRING database in 2021: customizable protein–protein networks, and functional characterization of user-uploaded gene/measurement sets. *Nucleic Acids Res.* 49, D605–D612. <https://doi.org/10.1093/nar/gkaa1074>.
- Szklarczyk, D., Morris, J.H., Cook, H., Kuhn, M., Wyder, S., Simonovic, M., Santos, A., Doncheva, N.T., Roth, A., Bork, P., et al. (2016). The STRING database in 2017: quality-controlled protein–protein association networks, made broadly accessible. *Nucleic Acids Res.* 45, D362–D368. <https://doi.org/10.1093/nar/gkw937>.
- Van der Hoek, K.H., Eyre, N.S., Shue, B., Khantisitthiporn, O., Glab-Ampi, K., Carr, J.M., Gartner, M.J., Jolly, L.A., Thomas, P.Q., Adikusuma, F., et al. (2017). Viperin is an important host restriction factor in control of Zika virus infection. *Sci. Rep.* 7, 4475. <https://doi.org/10.1038/s41598-017-04138-1>.
- Xie, Z., Jiao, H., Xiao, H., Jiang, Y., Liu, Z., Qi, C., Zhao, D., Jiao, S., Yu, T., Tang, X., et al. (2020a). Generation of pRSAD2 gene knock-in pig via CRISPR/Cas9 technology. *Antiviral Res.* 174, 104696. <https://doi.org/10.1016/j.antiviral.2019.104696>.
- Xie, Z., Jiao, H., Xiao, H., Jiang, Y., Liu, Z., Qi, C., Zhao, D., Jiao, S., Yu, T., Tang, X., et al. (2020b). Generation of pRSAD2 gene knock-in pig via CRISPR/Cas9 technology. *Antiviral Res.* 174, 104696. <https://doi.org/10.1016/j.antiviral.2019.104696>.
- Xie, Z., Pang, D., Yuan, H., Jiao, H., Lu, C., Wang, K., Yang, Q., Li, M., Chen, X., Yu, T., et al. (2018). Genetically modified pigs are protected from classical swine fever virus. *PLoS Pathog.* 14, e1007193. <https://doi.org/10.1371/journal.ppat.1007193>.
- Xu, K., Zhou, Y., Mu, Y., Liu, Z., Hou, S., Xiong, Y., Fang, L., Ge, C., Wei, Y., Zhang, X., et al. (2020). CD163 and pAPN double-knockout pigs are resistant to PRRSV and TGEV and exhibit decreased susceptibility to PDCoV while maintaining normal production performance. *Elife* 9, e57132. <https://doi.org/10.7554/eLife.57132>.
- Yan, Q., Yang, H., Yang, D., Zhao, B., Ouyang, Z., Liu, Z., Fan, N., Ouyang, H., Gu, W., and Lai, L. (2014). Production of transgenic pigs over-expressing the antiviral gene Mx1. *Cell Regen.* 3, 11. <https://doi.org/10.1186/2045-9769-3-11>.
- Zhang, X., Di, C., Chen, Y., Wang, J., Su, R., Huang, G., Xu, C., Chen, X., Long, F., Yang, H., and Zhang, H. (2020). Multilevel regulation and molecular mechanism of poly (rC)-binding protein 1 in cancer. *FASEB J.* 34, 15647–15658. <https://doi.org/10.1096/fj.202000911R>.
- Zhao, Y., Wang, T., Yao, L., Liu, B., Teng, C., and Ouyang, H. (2016). Classical swine fever virus replicated poorly in cells from MxA transgenic pigs. *BMC Vet. Res.* 12, 169. <https://doi.org/10.1186/s12917-016-0794-5>.
- Zheng, G., Li, L.-F., Zhang, Y., Qu, L., Wang, W., Li, M., Yu, S., Zhou, M., Luo, Y., Sun, Y., et al. (2020). MERTK is a host factor that promotes classical swine fever virus entry and antagonizes innate immune response in PK-15 cells. *Emerg. Microbes Infect.* 9, 571–581. <https://doi.org/10.1080/22221751.2020.1738278>.
- Zhou, B. (2019). Classical swine fever in China—an update minireview. *Front. Vet. Sci.* 6, 187. <https://doi.org/10.3389/fvets.2019.00187>.
- Zhou, X., You, F., Chen, H., and Jiang, Z. (2012). Poly(C)-binding protein 1 (PCBP1) mediates housekeeping degradation of mitochondrial antiviral signaling (MAVS). *Cell Res.* 22, 717–727. <https://doi.org/10.1038/cr.2011.184>.

STAR★METHODS

KEY RESOURCES TABLE

REAGENT or RESOURCE	SOURCE	IDENTIFIER
Antibodies		
Rabbit polyclonal anti-PCBP1 antibody	BOSTER	Cat# A02636-1
Mouse monoclonal anti-GAPDH antibody	BEYOTIME	Cat# AG019; RRID:AB_2861160
HRP-conjugated goat anti-rabbit/mouse IgG (H + L)	BOSTER	Cat# BA1056
Pig polyclonal anti-E2 antibody	(Li et al., 2016)	N/A
FITC-labeled goat anti-pig IgG	SIGMA	Cat# F1638; RRID:AB_259436
Bacterial and virus strains		
CSFV Shimen	(Xie et al., 2018)	N/A
PRV bartha-k61	Jilin Zhengye Biological Products CO., LTD	N/A
PEDV attenuated vaccine	Jilin Zhengye Biological Products CO., LTD	N/A
Chemicals, peptides, and recombinant proteins		
T7 endonuclease	NEB	Cat# M0302
TRNzol Universal Reagent	TIANGEN	Cat# DP424
Polyethylenimine (PEI)	SIGMA	Cat# 764965-1G
Critical commercial assays		
pX330 plasmid	Addgene	Cat# 42230
BTX-ECM 2001	BTX	Cat# 45-2046
2-mm gap cuvette	BTX	Cat# 45-0141
FastKing RT Kit	TIANGEN	Cat# KR116-02
SuperReal PreMix Plus (SYBR Green)	TIANGEN	Cat# FP205-02
Cell Lysis Buffer for Western and IP	BEYOTIME	Cat# P0013
Protease Inhibitor Cocktail	BEYOTIME	Cat# P1005
Cell Counting Kit-8	BOSTER	Cat# AR1160
Experimental models: Cell lines		
Porcine kidney cell line-15 (PK-15)	ATCC	Cat# CCL-33
Oligonucleotides		
PCBP1_F: 5'-AGACTTGACCACGTAACGAGCC-3' (PCR)	This study	N/A
PCBP1_R: 5'-CTCTCGGGATCTCTTTGATCT-3' (PCR)	This study	N/A
PCBP1_DL_F: 5'-TCACCGAGTGTGTCAAGCAG-3' (qPCR)	This study	N/A
PCBP1_DL_R: 5'-CATGGGTGGCATGAGGGTAG-3' (qPCR)	This study	N/A
Sg97_Forward: 5'-GTCGGTTAAGAGGATCCGCG-3' (sgRNA targeting sequence)	This study	N/A
Sg97_Reverse: 5'-CGCGGATCTCTTAACCGAC-3' (sgRNA targeting sequence)	This study	N/A
Sg95_Forward: 5'-CGCTATGATCATCGACAAGC-3' (sgRNA targeting sequence)	This study	N/A
Sg95_Reverse: 5'-GCTTGTGCGATGATCATAGCG-3' (sgRNA targeting sequence)	This study	N/A
CSFV_DL_F: 5'-CTAGCCATGCCACAGTAGGA-3' (qPCR)	This study	N/A

(Continued on next page)

Continued

REAGENT or RESOURCE	SOURCE	IDENTIFIER
CSFV_DL_R: 5'-CTCCATGTGCCATGTACAGCA-3' (qPCR)	This study	N/A
PEDV_DL_F: 5'-TCTCACTACTTCTGTGATGGGC-3' (qPCR)	This study	N/A
PEDV_DL_R: 5'- GATGAAGCATTGACTGAACGAC-3' (qPCR)	This study	N/A
PRV_DL_F: 5'-GGTTCAACGAGGGCCAGTACCG-3' (qPCR)	This study	N/A
PRV_DL_R: 5'-GCGTCAGGAATCGCATCACGT-3' (qPCR)	This study	N/A
GAPDH_F: 5'-GCCATCACCATCTTCCAGG-3' (qPCR)	This study	N/A
GAPDH_R: 5'-TCACGCCATCACAAACAT-3' (qPCR)	This study	N/A
IFNalpha_DL_F: 5'-GCCTCTGCACCAGTTCTACA-3' (qPCR)	This study	N/A
IFNalpha_DL_R: 5'-TGCATGACACAGGCTTCCA-3' (qPCR)	This study	N/A
IL6-DL_F: 5'-CTGGCAGAAAACAACCTGAACC-3' (qPCR)	This study	N/A
IL6-DL_R: 5'-TGATTCTCATCAAGCAGGTCTCC-3' (qPCR)	This study	N/A
ISG15_DL_F: 5'-ACTGCATGATGGCATCGGAC-3' (qPCR)	This study	N/A
ISG15_DL_R: 5'-CAGAACTGGTCAGCTTGAC-3' (qPCR)	This study	N/A
ISG56_DL_F: 5'-TTAGAAAACAGGGTCTTGGAGGAG-3' (qPCR)	This study	N/A
ISG56_DL_R: 5'-CGTAAGGTAATACAGCCAGGCATA-3' (qPCR)	This study	N/A
RSAD2_DL_F: 5'-AAGCAGAGCAGTTTGTTCAGC-3' (qPCR)	This study	N/A
RSAD2_DL_R: 5'-TTCCGCCCGTTTCTACAGT-3' (qPCR)	This study	N/A
MXA_DL_F: 5'-GATCCGGCTCCACTTCCAAA-3' (qPCR)	This study	N/A
MXA_DL_R: 5'-CTCTGTGCTGGTGCTACT-3' (qPCR)	This study	N/A
CDC5L_DL_F: 5'-GTGGGACAACCTCCCAAACCA-3' (qPCR)	This study	N/A
CDC5L_DL_R: 5'-GGAAGGCCCAACAAGCCTAA-3' (qPCR)	This study	N/A
ELAVL1_DL_F: 5'-GGTTCCTCCGAGCCATTAC-3' (qPCR)	This study	N/A
ELAVL1_DL_R: 5'-GAACCTGAATCTCTGCGCCT-3' (qPCR)	This study	N/A
PPIL3_DL_F: 5'-ATCACCTATGGCAAGCAGCC-3' (qPCR)	This study	N/A
PPIL3_DL_R: 5'-TACTGAGCAAATGGGTTGGCA-3' (qPCR)	This study	N/A
SRSF1_DL_F: 5'-CAACGATTGCCGATCTACG-3' (qPCR)	This study	N/A
SRSF1_DL_R: 5'-TCCTCGAACTCAACGAAGGC-3' (qPCR)	This study	N/A
TRA2B_DL_F: 5'- GAACTACGGCGAGCGGGAAT-3' (qPCR)	This study	N/A
TRA2B_DL_R: 5'-CTTGGAGCGAGACCTTGCG-3' (qPCR)	This study	N/A
PCBP2_DL_F: 5'-CCTGCTAGTCAGTGTGGCTC-3' (qPCR)	This study	N/A
PCBP2_DL_R: 5'-GTCTCCAACATGACCACGCA-3' (qPCR)	This study	N/A
Recombinant DNA		
pX330-sg95	This study	N/A
pX330-sg97	This study	N/A
pcDNA3.1-PCBP1	This study	N/A
Software and algorithms		
GraphPad Prism 8	GraphPad Software	N/A
Fiji software	NIH	ImageJ (nih.gov)

RESOURCE AVAILABILITY

Lead contact

Further information and requests for resources and reagents should be directed to and will be fulfilled by the lead contact, Prof. Zicong Xie (xzc@jlu.edu.cn).

Materials availability

This study did not generate new unique reagents.

Data and code availability

- Data reported in this paper will be shared by the [lead contact](#) upon request.
- This paper does not report original code.
- Any additional information is available from the [lead contact](#) upon request.

EXPERIMENTAL MODEL AND SUBJECT DETAILS

Cells and viruses

Porcine kidney cell line-15 (PK-15) cells (ATCC Number: CCL-33) were cultured in Dulbecco's modified Eagle's medium (DMEM, Gibco) supplemented with 5% fetal bovine serum (FBS), 10 Unit/mL penicillin, 10 μ g/mL streptomycin, 1% Non-Essential Amino Acids (NEAA, Gibco), and 2 mM L-Glutamine (Gibco). Primary porcine fetal fibroblasts (PFFs) were cultured in DMEM containing 15% FBS, 10 Unit/mL penicillin, 10 μ g/mL streptomycin, 1% NEAA, and 2mM L-Glutamine. All cells were grown in an atmosphere of 5% CO₂ at 37°C.

The sex of PK-15 cells and PFFs are female.

All experiments about viruses were conducted in BSL II laboratory. CSFV Shimen strain (Xie et al., 2018) and PRV bartha-k61 strain were used and maintained at -80°C. PEDV attenuated vaccine (strain CV777) was purchased from Jilin Zhengye Biological Products CO., LTD. All attenuated virus in dry powder form was stored at 4°C and the stock solution was preserved at -80°C.

METHOD DETAILS

Plasmid construction

CrRNA sequence was searched through the porcine *PCBP1* gene using the CHOPCHOP webtools (<https://chopchop.cbu.uib.no/>). CACC sequence was added at 5' end of the top strand of selected crRNA sequences and AAAC was added at 5' end of the bottom strand. These sgRNA oligonucleotides were synthesized by Comate Bioscience CO., LTD and ligated into linear pX330 plasmid (42230, Addgene) digested by Bbs I to form the intact targeting plasmids. The pHA-PCBP1-His plasmid was generated by cloning PCBP1 CDS sequence flanked by HA and His tag into pcDNA3.1 (+). The plasmids used in this research were confirmed by DNA sequencing.

Electroporation and generation of knock out cell clones

Approximately 30 μ g pX330 plasmids containing crRNAs targeting different region of porcine PCBP1 gene were electrotransfected into $\sim 3 \times 10^6$ PFFs using Neon Transfection System (invitrogen). The specified parameters applied to PFFs uniquely were as follows: 1260 voltage, 30ms, 1 pulse. Similarly, 30 μ g pX330 plasmids were introduced into $\sim 3 \times 10^6$ PK-15 cells resuspended in 300 μ L Opti-MEM (Gibco) in 2 mm gap cuvettes using BTX-ECM 2001. The parameters were as follows: 300 voltage, 1 ms, 3 pulses, 1 repeat.

The PFFs and PK-15 cells were seeded into ten 100mm dishes after 48 h post-transfection, and the inoculation density per dish was 2000 cells on average. The cell clones were picked and continually cultured in 24-well plates. Forty percent of one well were digested for 2 min at 37°C and lysed with 10 μ L NP-40 lysis buffer (10 mM Tris-HCl pH 8.3, 50 mM KCl, 1.5 mM MgCl₂, 1% NP-40, and 1% protease K) for 1 h at 56°C and 10 min at 95°C after each clone reaching into 80% confluency. The lysate was used as PCR template and subjected to Sanger sequencing. The positive PK-15 clones were propagated into 100 mm dishes one step at a time. The positive PFFs clones were grown on 24-well plates until SCNT.

T7E1 assay

Genomic DNA of positive PK-15 cell clones was extracted using TIANamp Genomic DNA Kit (TIANGEN). And a conventional PCR was performed as follows: 95°C for 4 min; 95°C for 30 s, 59°C for 30s, 72°C for 30s, for 35 cycles; 72°C for 5 min; hold at 4°C. The PCR products were purified using QIAquick PCR Purification Kit (Qiagen). Approximately 200 ng purified PCR products in the presence of 10 \times NEB Buffer 2 were

reannealed using following cycles: 95°C for 5 min; 95-85°C at the rate of $-2^{\circ}\text{C}/\text{s}$, 85-25°C at the rate of $-0.1^{\circ}\text{C}/\text{s}$; hold at 4°C. Then, 1 μL T7 endonuclease was added to each sample and the reactions were incubated at 37°C for 15 min. the reaction mixtures were then analyzed on a 2% agarose gels.

Virus infection

Cells were seeded in 6-well plates before viral infection. For CSFV and PRV infection, cells were replaced with fresh culture medium after incubating for 1 h at corresponding multiplicity of infection (MOI). For attenuated PEDV infection, the absorption phase was maintained for 1 h at a MOI of 10 in the presence of 10 $\mu\text{g}/\text{mL}$ trypsin, after which the maintenance medium containing 10 $\mu\text{g}/\text{mL}$ trypsin was added. At various hpi, samples containing viral genome were harvested and stored at -80°C until use.

Plasmids transfection

Approximately 3×10^5 cells were seeded in 6-well plate and transfected with corresponding plasmid (3 μg /well) using PEI (SIGMA) at 1:2 ratios of DNA to PEI when cells were grown to 60–70% confluency. At 48 h post transfection, cells were infected with CSFV (MOI = 1) and viral replication was detected by RT-qPCR.

Viral genome extraction and real-time quantitative PCR

As for CSFV, total intracellular RNA was extracted from CSFV-infected PK-15 cell pellet and extracellular RNA was extracted from according supernatant using TRNzol Universal Reagent (TIANGEN). Around 2 μg RNAs were performed to reverse transcript to the first-strand cDNAs using FastKing RT Kit (TIANGEN) according to manufacturer's instruction. As for PEDV, the monolayer of virus-infected cells was scraped by cell scraper within the culture medium and 200 μL suspension was aspirated and mixed with 800 μL TRNzol Universal Reagent. The subsequent reverse transcription was consistent with the above. As for PRV, the virus-infected material was obtained in the same manner as PEDV. And the PRV genome within 200 μL suspension was extracted by TIANamp Virus DNA/RNA Kit (TIANGEN). All cDNAs and viral genome were -20°C . Primers used to amplify corresponding genes were displayed in key resources table.

To detect the accurate viral copy number in virus-infected materials, a standard curve was generated with 10-fold serial dilutions ranging from 10^9 to 10^3 . The quantitative PCR was performed using Quantagene q225 (KUBOTECHNOLOGY) with SuperReal PreMix Plus (TIANGEN) according to the manufacturer's instruction. To check the relative expression of predicted genes or genes associated with porcine *PCBP1*, the housekeeping gene glyceraldehyde 3-phosphate dehydrogenase (*GAPDH*) was selected as reference gene and the mRNA expression was normalized to *GAPDH* using the $2^{-\Delta\Delta\text{Ct}}$ method.

Western Blot

The cells were washed in ice-cold phosphate-buffered saline (PBS) and lysed in Cell Lysis Buffer for Western and IP (P0013, BEYOTIME) in the presence of 1mM PMSF (AR1192, BOSTER) and 1% Protease Inhibitor Cocktail (P1005, BEYOTIME). The protein concentrations were measured with the BCA assay Kit (AR1189, BOSTER) and 40 μg proteins were diluted in 5 \times SDS-PAGE Loading Buffer (AR1112, BOSTER) at 95°C for 10 min. Subsequently, the samples boiled were resolved on the artificial 4–12% SDS-PAGE gel and the proteins were transferred to nitrocellulose membranes. The membranes were blocked with 5% skim milk dissolved in TBST for 2 h at room temperature. Primary antibodies for immunoblotting were as follows: rabbit anti-PCBP1 (1:2000, BOSTER A02636-1) and mouse anti-GAPDH (1:1000, BEYOTIME AG019). Membranes were subsequently washed in TBST and then incubated with horseradish peroxidase-conjugated goat anti-rabbit/mouse IgG (H + L) (1:5000, BOSTER BA1056). Ultimately, membranes were imaged with the ultra-sensitive ECL chemical luminescence ready-to-use kit (BOSTER AR1197) using Azure c600 (AZUREBIOSYSTEMS). The corresponding protein bands were normalized to GAPDH band density using Fiji.

Binding, entry, and replication assay

Cells were seeded in 12-well plates and the confluency reached 95% before CSFV infection. Next, cells were inoculated with CSFV at 4°C for 1 h to allow virus binding without internalization and then cells were washed with ice-cold PBS three times so that unbound virus particles were removed. The culture medium was replaced with fresh complete medium and cells were subsequently shifted to 37°C with 5% CO_2 for 0 h (binding), 1 h (entry), and 24 h (replication). For binding assay, cells were immediately pelleted for RT-qPCR. For

entry assay, cells were washed with ice-cold PBS three times to remove uninternalized virions on cell surface and collected for RT-qPCR after 1h. For replication assay, cells were collected after 24 h for RT-qPCR.

IFA

The primary fibroblasts were seeded into 24-well plates with four replicates per sample. The cells, reaching 80% confluency, were infected with CSFV (MOI = 1). At 1 h post-inoculation, cells were replaced with fresh CSFV-free culture medium. After 48h infection, cells were washed with cold PBS and fixed in 4% paraformaldehyde for 30 min at room temperature. The primary antibodies and fluorophore-conjugated antibody were as follows: pig anti-E2 antibody (PAb) (1:100) (Li et al., 2016), FITC-labeled goat anti-pig IgG (No. F1638, SIGMA). Samples were incubated with primary antibodies for 1 h in cold blocking buffer (10% FBS in PBS) at 37°C, followed by three washes in PBS and incubated with secondary antibodies in a dark, humidified chamber for 1 h at 37°C. Before imaged with EVOS f1 fluorescence microscope, samples were washed five times with PBS.

SCNT

The PCBP1 deficient PFFs were used for somatic cell nuclear transfer as described previously (Lai et al., 2002). The positive cells were injected into the perivitelline cytoplasm of enucleated oocytes to form reconstructed embryos. Subsequently, reconstructed embryos were surgically transferred into the oviducts of surrogate females on the first day of estrus after activated and cultured for approximately 18 h in embryo culture medium. Pregnancy status was detected using ultrasound scanner between 30 and 35 days post-transplantation. To monitor the blastocyst formation rate and developmental viability, a part of activated embryos was continually cultured for 7 days.

Isolation of primary porcine fibroblast

The tail tips from PCBP1-deficient and WT piglets were cut into small pieces, followed by digested with the fresh culture medium containing 20% FBS in the presence of 25 Unit/mL DNase I and 200 Unit/mL type IV collagenase for 4 h at 39°C. Then, dissociated primary cells and tail pieces were continually cultured for 4–5 days. The isolated tail fibroblasts were cryopreserved at –80°C for 24 h, followed by moved to liquid nitrogen for long term storage.

Cell viability assay

Cell viability was evaluated with the Cell Counting Kit-8 (AR1160, BOSTER) according to the manufacturer's instruction. Briefly, the PCBP1 KO PFFs or WT cells were seeded into 96-well plates at a density of 5×10^3 cells/well. The cells were replaced with fresh culture medium containing 10% CCK-8 reagent until attached to plates. An additional inoculation were applied for 1 h at 37°C. The absorbance at 450nm was measured using TECAN Infinite 200 PRO.

QUANTIFICATION AND STATISTICAL ANALYSIS

Statistical analysis was performed using GraphPad Prism 8.0 software. Student t tests were used to compare two groups. $p < 0.05$ was considered statistically significant.